Fragment-based drug discovery approaches towards novel 5-HT3 receptor ligands

Verheij, M.H.P.

2012

document version
Publisher's PDF, also known as Version of record

CHAPTER 4

SMALL AND COLORFUL TESSERAE MAKE BEAUTIFUL MOSAICS: FRAGMENT-BASED CHEMOGENOMICS

Chris de Graaf, Henry F. Vischer, Gerdien E. de Kloe, Albert J. Kooistra, Saskia Nijmeijer, Martien Kuijer, Mark H. P. Verheij, Paul England, Jacqueline E. van Muijlwijk-Koezen, Rob Leurs and Iwan J. P. de Esch

Abstract

Smaller tesserae with a wide variety of colours make a higher resolution mosaic. In much the same way, smaller chemical entities that are structurally diverse are better able to interrogate protein binding sites. This *feature article* describes the construction of a diverse fragment library and the analysis of six protein targets belonging to three diverse target classes (GPCRs, LGICs, and kinases) using chemogenomics approaches. Biochemical fragment screening yielded fragment hit rates varying between 1 and 10%. Analysis of the different hit sets shows that fragment screening can be used to gain new insights into the atomic details of protein-ligand interactions and selectivity issues, for example by identifying ligand-affinity cliffs and molecular selectivity switches.

Introduction

Fragment-based drug discovery (FBDD) has obtained a significant role in modern drug discovery process.[1] The 'small is beautiful' concept has stimulated fragment library design [2], the development of highly sensitive screening methods [3, 4] and structure-based optimization strategies.[5] Key advantage of FBDD is that the respective chemical space described by low molecular weight compounds is much smaller than for drug-like compounds. In addition, the lower complexity of small fragments is believed to increase the chance of a good match between ligand and protein, as was elegantly described in a hallmark publication by Hann and co-workers.[6] It is therefore anticipated that fragments are compatible with more than one target. This is illustrated by the fact that FBDD is considered to be the method of choice for the design of ligands with multi-target profiles.[7] Furthermore, substructure analysis of bioactive molecules have identified privileged substructures which are abundant in the ligands of specific protein classes (e.g., 2-phenyl-indole, spiro-piperidine-indane, and 2-tetrazole-biphenyl substructures observed in ligands of different G protein-coupled receptors [8, 9]), or are predisposed to bioactivity in general (e.g., biphenyl substructure [10]). In a recent study, little specificity was observed in fragments selected by structure-based virtual screening for two unrelated β-lactamases (CTX-M and AmpC).[11] Teotico et al. argue that the lack of selectivity is due to the ability of fragments to adapt to different protein environments and that upon ligand optimization selectivity is automatically gained.[11] Fragment screening studies against panels of (homologous) proteins on the other hand have been successfully used to identify *selective* fragments for aspartate semialdehyde dehydrogenases from different microbial species [12], and selective fragments for a panel of 12 protein kinases.[13] Yet, an opposite result was obtained with the screening of a small library of 150 fragments against five protein targets, which yielded many non-selective low affinity hits; 15% of the fragments interacted with 4 out of 5 proteins.[14] The relatively high hydrophobicity of this set of promiscuous hits suggest that target cross-reactivity in this case mainly is the result of binding driven by desolvation.[15] Clearly, it is important to design a fragment library with optimal physico-chemical properties that strikes the right balance with respect to sufficiently high hit rates for a diverse set of protein targets while obtaining selective interactions. This feature article reviews the construction of a structurally diverse fragment library and describes the screening results and cheminformatics analysis. The fragment-based chemogenomics analysis of (four) G protein-coupled receptors (bioaminergic receptors ADRB2, H_1R, H_3R, and H_4R) as well as two unrelated protein targets, including a Cys-loop ligand-gated ion channel (serotonin receptor 5-HT_3R), and a Ser/Thr kinase (PKA) is described. Using resource- and time-efficient biochemical screening, diverse sets of fragment hits were obtained for all targets from a proprietary, chemically diverse library of 1010 fragments. Fragment bioaffinity profiles across related protein targets are explored to identify ligand affinity cliffs, while screening data comparisons between unrelated targets identified

molecular selectivity switches. We suggest that these cliffs and switches can be used to obtain new insights into the atomic details of protein-ligand interactions.

Library Design

The properties of the fragment library will determine the results of the chemogenomics studies, warranting a detailed discussion about fragment library construction. In the first step of the library design workflow (step 1, Figure 1a), fragments were identified based on a set of properties that was inspired by the rule-of-three selection criteria [16], i.e., number of heavy atoms ≤ 22, logP < 3, number of H-bond donors ≤ 3, number of H-bond acceptors ≤ 3, number of rotatable bonds ≤ 5, number of rings ≥ 1. Most of the fragments identified were originally synthesized as intermediate compounds in synthetic routes towards drug-like molecules, thereby implicitly offering convenient chemical handles for further synthetic exploration. Fragments that contain functional groups that are not compatible with pharmacological or biophysical screening assay conditions were removed, following published rules (step 2).[17] Next, a scaffold diversity analysis [18] was used to evaluate the resulting fragment set and identified scaffolds that were over-represented, e.g., pyridines and piperazines. For these scaffolds, representative fragments with high cyclicity [18] were selected (step 3). Fragments with stocks smaller than 5 mg also were excluded (step 4). The scaffold diversity analysis then identified under-represented scaffolds and subsequently 81 novel scaffolds (117 fragments) were purchased (step 5). Finally, the library consisted of a diverse set of 1010 fragment-like molecules.

Diversity of the fragment library

Figure 1b shows the distribution plots of several physico-chemical properties of the fragment library. Figure 1b shows that the mean molecular weight is just above 200 Da (211 ± 47). Most reported fragment libraries avoid fragments below 100 Da.[2] The upper limit of 22 heavy atoms resulted in quite some fragments above 250 Da, which is the upper limit for e.g. the Astex and Vernalis fragment libraries.[2] The relatively high molecular weight cut-off was implemented to accommodate higher complexity fragments that also contain halogen atoms (attractive for synthetic exploration and X-ray analysis). In addition, the library was designed to be compatible with biochemical fragment screening approaches and these are typically less sensitive than biophysical screening technologies. The diversity of the fragment library was assessed by scaffold diversity analysis as fragments are represented by the complexity of their scaffolds (described by six descriptors [18]) and the ratio between scaffolds and side chains. This Scaffold-based Classification Approach (SCA) results in plots (Figure 1c and d) that have been successfully used to visualize the diversity of screening libraries, for example by scientists from Zobio and Pyxis Discoveries.[19, 20] Comparison of the chemical space covered by the constructed fragment library with the chemical space of commercially available fragments (e.g., the VitasM Lab commercial fragment library [21], 8326 compounds, Figure 1c) and bioactive fragment-like molecules (13.375 cpds identified in the chEMBL database [22]) (Figure 1d) demonstrates the

diversity of the fragment library used in the current study. Only very complex fragments and complex fragments with lower cyclicity values are not covered. The lower left area in the SCA plots represents small aliphatic ring systems, e.g. cyclopropyl and cyclobutyl scaffolds. The current library is underrepresented in this area of scaffold space. While acknowledging this specific caveat, no fragments were purchased to fill this chemical space as the synthesis of such fragments can be complicated with respect to chemical reactivity and chiral centers. Instead, the analysis did lead to renewed interest in proprietary synthetic chemistry that leads to cyclobutyl [23] and cyclopropyl.[24]

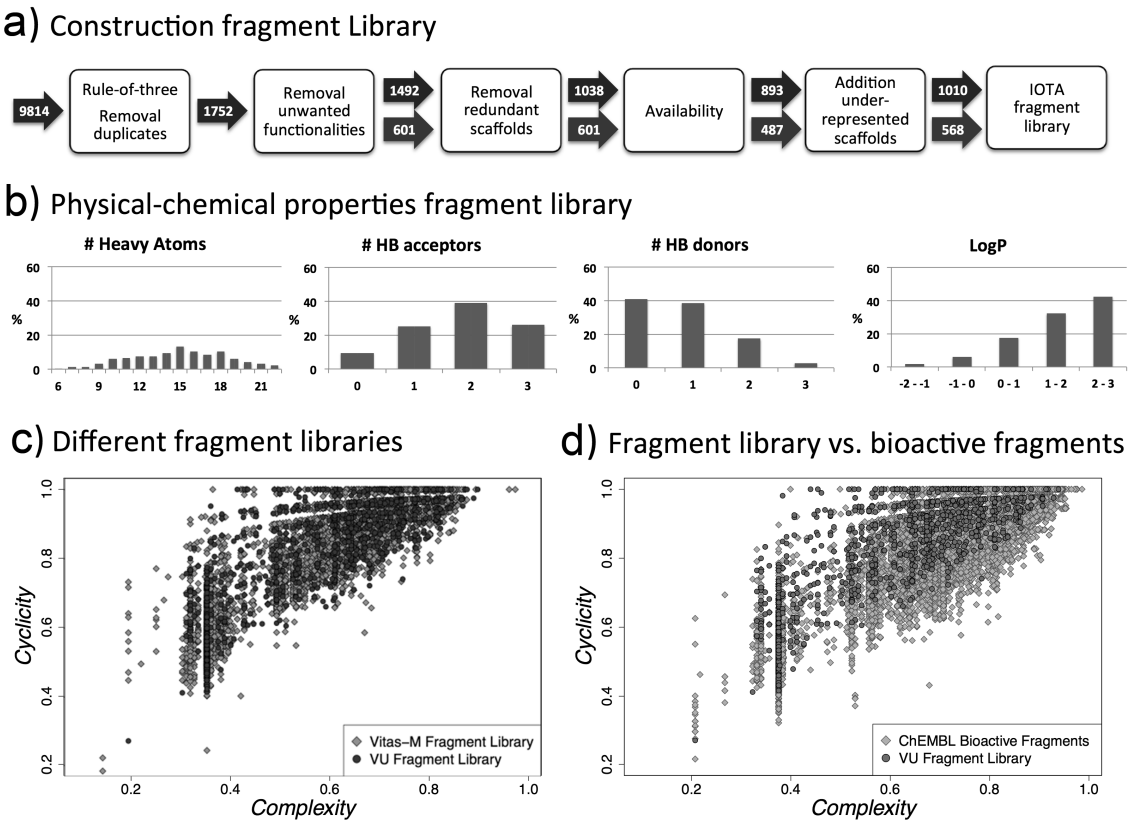

Figure 1. *(a) Flow scheme construction of the fragment library, top arrows represent total number of compounds, bottom arrows represent total number of scaffolds. b) Distribution of number of heavy atoms, Log (P) values, number of H-bond donors, number of H-bond acceptors, and number of rotatable bonds of the molecules in the fragment library. Comparison SCA plots of VU fragment library with (c) the VitasM 8326 fragment library and (d) bioactive fragments from ChEMBLdb.*

Fragment-based chemogenomics

Fragment screening results

To illustrate the chemogenomics approaches, a selection of six targets is described. As with any chemogenomics study, there is an intrinsic complication when comparing a variety of drug targets, e.g., different assay formats and compound concentrations. Nevertheless, the screening results represent the probing of respective binding sites with fragments. Hits for all six targets were found, with hit rates varying from 1-10% (Table 1). High hit rates were obtained, especially for targets for which already many fragment-like molecules have been described in literature, including 5-HT_3R, H_3R, and H_4R (Table 1). Also for these targets, however, novel fragment scaffolds were identified, as defined by their Tanimoto score (Table 1). Interestingly, also for ADRB2 [25], a target that mainly binds the phenylethanolamine and phenoxypropanolamine ligands [9], a novel fragment-like molecules has been identified (e.g., selective ADRB2 ligand 1, Table 2, Figure 2g, Figure 3b). This demonstrates the potential of fragment screening in identifying new (and selective) bioactive lead compounds for drug development.

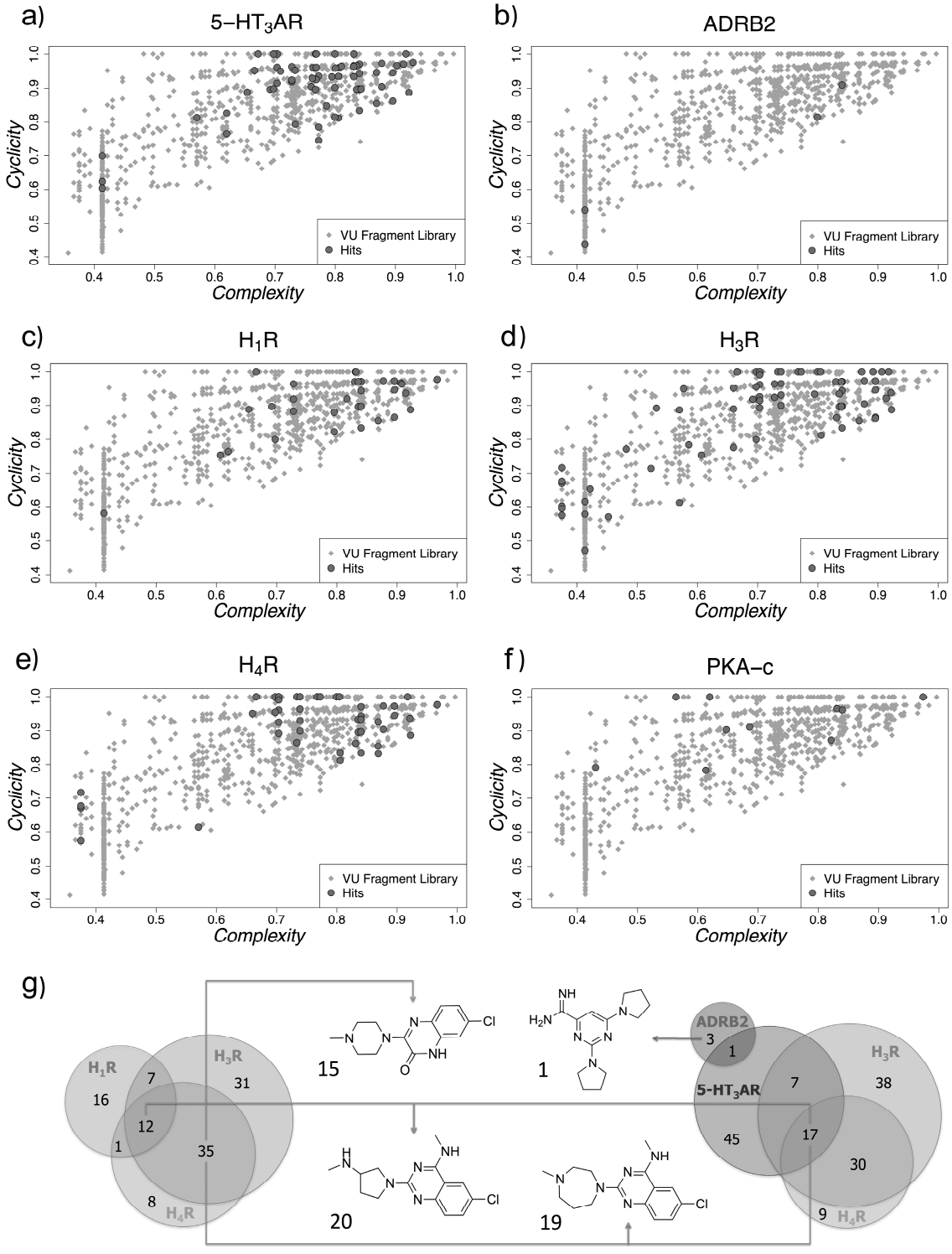

Figure 2. *SCA plots displaying active (dark grey dots) and inactive (light grey dots) fragments for 5-HT_3R (a), ADRB2 (b), H_1R (c) , H_3R (d) , H_4R (e), PKA-C (f). Panel G shows examples of fragment ligand overlap (g) within receptor subtypes (H_1R/H_3R/H_4R) and across receptor subtypes (5-HT_3R, H_3R, H_4R, ADRB2).*

Table 1. Hit-rates, novelty and specificity of hits, number of known fragment-like ligands for a target.

	# Fragment hits[a]	# Novel hits[a]	# Target-specific hits (%)[c]	# Known fragment-like ligands (%)[d]
Library	1010	-	-	-
5-HT_3R[e]	70[f]	56	41 (59%)	168 (36%)
ADRB2[f]	4[g]	1 (25%)	3 (75%)	21 (2%)
H_1R[g]	36[h]	27 (75%)	12 (33%)	48 (6%)
H_3R[h]	87[i]	24 (28%)	26 (30%)	186 (8%)
H_4R[i]	59[j]	16 (27%)	6 (10%)	100 (22%)
PKA-c[j]	10[k]	10 (100%)	10 (100%)	18 (8%)
Single target	98	77 (79%)	-	-
Two targets	44	14 (30%)	-	-
Three targets	12	0 (0%)	-	-
Four targets	11	0 (0%)	-	-
Total hits	165	91 (55%)	98 (59%)	553 (11%)

[a]More than 50% radioligand displacement, unless stated otherwise; [b]Fragment hits with ECFP-4 Tanimoto similarity < 0.4[26] to any known ligand for the particular target in the chEMBLdb (omitting those entries that refer to VU University's publications that describe recent target-centric fragment library screening studies [27]) and); [c]Unique hits for the particular target; [d]Number of active ligands in chEMBL database (omitting those entries that refer to VU University's publications that describe recent target-centric fragment library screening studies [27]; which obey fragment rules as applied for our own fragment library, as described in the Methods, full overview given in Table S-1; [e]Displacement of [^{3}H]granisetron at 100µM using membranes of HEK293 cells expressing the human 5-$HT_{3A}R$ [28]; [f]Displacement of [^{3}H]-Dihydroalprenolol at 30µM using membranes of HEK293T cells expressing ADRB2 [29]; [g]Displacement of [^{3}H]-pyrilamine at 10µM using membranes of HEK293T cells expressing H_1R [30]; [h]Displacement of [^{3}H]-NAMH at 10µM using membranes of HEK293T cells expressing H_3R [30]; [i]Displacement of [^{3}H]-histamine at 10µM using membranes of HEK293T cells expressing H_4R [30]; [j]Displacement of [^{3}H]-ATP at 10µM using the catalytic domain of PKA-c alpha.

The results of the screens are presented in SCA plots to illustrate the diversity of the hits. Figure 2 clearly shows that for all targets diverse sets of hits have been found, as the hits are scattered throughout scaffold space. Even when the hit rate is very low, in case of PKA-c (Figure 2f), hits are diverse in terms of cyclicity and complexity.

Physico-chemical properties of fragments match protein binding sites

Physico-chemical property distributions of the different fragment hit sets are presented in Figure 3a. Interesting complementarities can be found between the properties of fragment hits and their protein binding pockets. For example, histamine H_3R and H_4R receptor hits are relatively polar and contain a relatively high number of positively charged groups and (non-ionizable) H-bond donors (H_3R follows the same trend as H_4R), corresponding with the H_3R and H_4R ligand pharmacophore [31-33] that contains two H-bond donors. In the H_3R and H_4R binding pocket, these features are complementary to two negatively charged residues, $D^{3.32}$ and $E^{5.46}$, known to be important for the interaction of high affinity ligands (Figure 3d).[34-36] As a result of these strong non-desolvation related interactions [37] between ionizable H-bonding partners, many H_3R and H_4R ligands can bind the receptor with a high ligand-lipophilic efficiency (LLE, affinity diminished with log(P)).[38] This also explains the relatively low log(P) values of H_3R and H_4R ligands (Figure 3a). H_1R also contains $D^{3.32}$ [39, 40], but possesses a neutral $N^{5.46}$ residue [40, 41] (instead of the negatively charged $E^{5.46}$ in H_3R and H_4R) as well as an aromatic cluster of phenylalanines ($F432^{6.52}$/$F435^{6.55}$) [40, 42] which is not present in H_3R ($T375^{6.52}$/$M378^{6.55}$) and H_4R ($S320^{6.52}$/$T323^{6.55}$)[35, 36], as illustrated in Figure 3d-e. The requirements of the H_1R binding pocket [43] match H_1R fragment hits which contain a positively ionizable group and few non-ionizable H-bond donors (Figure 3a) in combination with rigid aromatic ring structures (data not shown) .

All hit fragments for ADRB2 contain a basic center (Figure 3a) that is likely to form an ionic interaction with the receptor's $D107^{3.32}$ [25], a conserved negatively ionizable residue that is considered an anchor for ligand binding in bioaminergic GPCRs (Figure 3d).[44, 45] Ligand binding to 5-$HT_{3A}R$ is largely determined by aromatic interactions like π-π stacking and cation-π interactions (W183, W195, Y141, Y143, Y153, Y234)[46-48], matching the abundance of rigid aromatic rings in 5-$HT_{3A}R$ fragments (Figure 3f).[27] Fragment hits on PKA-c are relatively small, hydrophobic, and rigid, and contain less ionizable groups (Figure 3a), corresponding with the hydrophobic binding pocket of protein kinases located around a conserved backbone binding motif.[49]

Relationship between fragment properties and protein cross reactivity

More than half of the fragments hits bind one specific target (Table 1). A substantial part of the hits however binds two (44 fragments), three (12 fragments) or even four (11 fragments) targets. There are no fragments that bind to all protein targets. While the significant fragment cross-reactivity between the H_3R and H_4R receptors (Figure 2g) is not surprising given their homology (31% at the protein level, 54% within the transmembrane domains) [33], it is interesting to see that fragment overlap between H_4R and unrelated proteins like $5HT_3R$ is significantly higher than between H_3R/H_4R versus H_1R histamine receptors (Figure 2g). These data are in line with our previous report on H_4R-$5HT_3R$ dual ligands.[27]

In contrast to other reports [14], there is no correlation in this dataset between non-selective fragments and fragment hydrophobicity (Figure 3b), indicating that the binding of the fragment hits identified in our screening studies is not primarily driven by unspecific desolvation energy as observed for larger bioactive molecules [15, 50] and in earlier fragment screening studies.[14] There is also no correlation between cross reactivity and low molecular weight as indicated by the analyses of Hopkins et al. (Figure 3b).[15, 50, 51] Moreover, the 10 ligands that interact with four targets have a relatively high molecular weight. The fragments that bind four targets ($H_1R/H_3R/H_4R/5\text{-}HT_3R$), like the quinoxaline (e.g., fragment 20 presented in Figure 2g and 3d) and quinazoline containing fragments, are relatively large and have complex scaffolds. There is however a bias for basic centers in the fragment hits, and especially in the fragments that bind several targets (Figure 3b). This is not surprising given the fact that five out of six targets are known to prefer basic ligands. Furthermore, earlier studies showed increase promiscuity for compounds that contain a basic or quaternary nitrogen atom, relative to neutral or acidic compounds.[15] In this dataset, the protein kinase PKA-c is the only targets that do not have a preference for positively ionizable ligands and bind many selective ligands (Table 1).

Very few hits were found for ADRB2. However, none of the seven hits bind any of the other GPCRs, while this receptor belongs to the same class of bioaminergic GPCRs as H_1R, H_3R, and H_4R. All these GPCRs bind their positively charged aminergic ligands via a conserved negatively charged $D^{3.32}$ residue at the center of the binding site (Figure 3c-e).[44, 52] The alcohol amine functional group present in almost all known ADRB2 ligands is complementary with a subpocket in ADRB2 formed by the $N312^{7.39}$ residue with $D113^{3.32}$ [25] (Figure 3c), which is unique for beta adrenergic receptors.[44] This could be an explanation for the observed selectivity, which demonstrates how subtle and local differences in binding pockets can strongly influence ligand selectivity, especially on a fragment level.

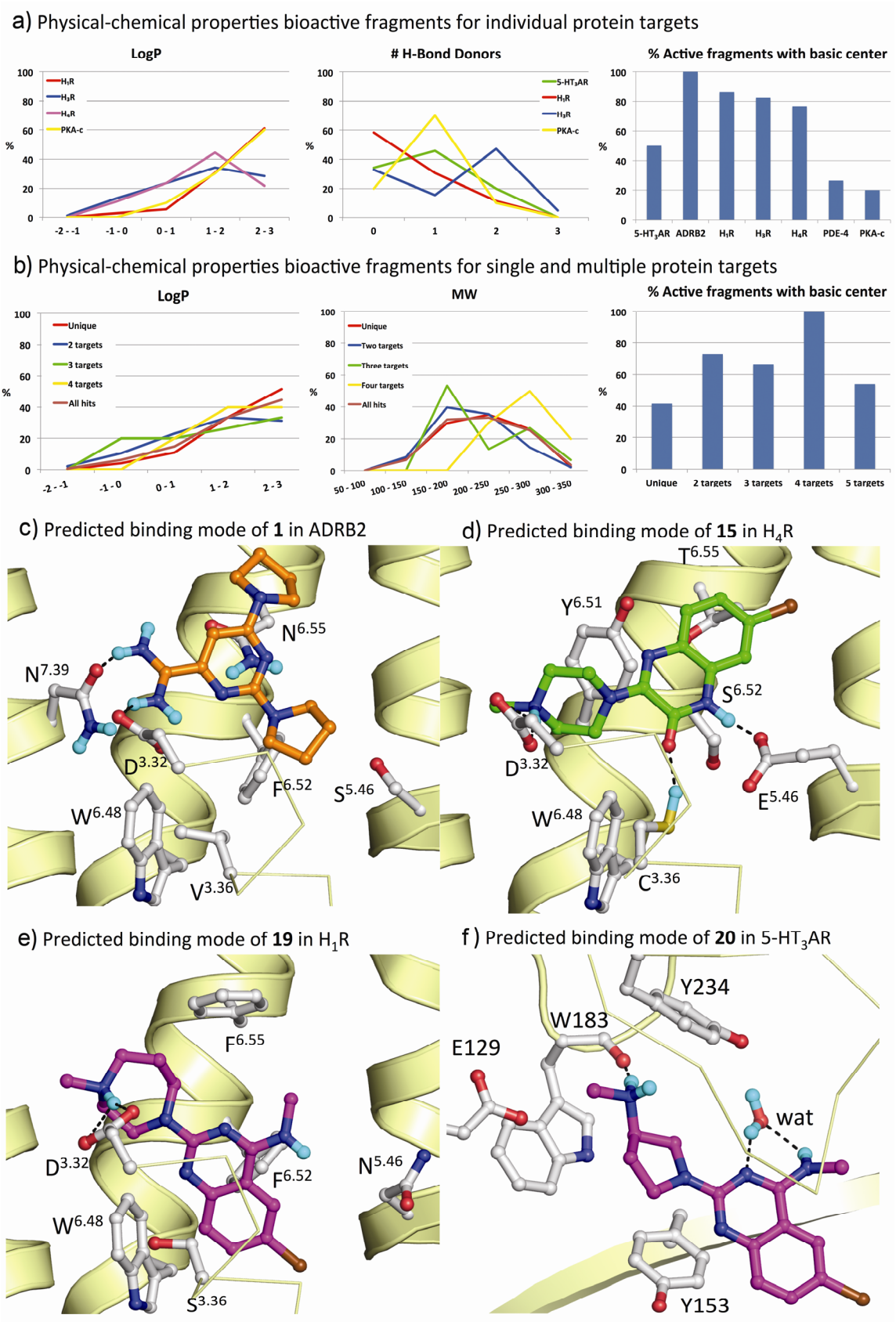

Figure 3. *(a) Histograms of physico-chemical property distributions of hits for different targets (red: H_1R, blue: H_3R, purple: H_4R, yellow: PKA-c, green: 5-HT_3AR). (b) Histograms of physico-chemical property*

distributions of selective and multitarget hits (red: unique, blue: 2 targets, green: 3 targets, yellow: 4 targets, brown: all hits). Molecular docking poses of (c) fragment 1 in ADRB2 crystal structure [25], (d) fragment 15 in H_1R crystal structure-based [43] H_4R homology model [36], (e) fragment 19 in H_1R crystal structure [43], and (f) fragment 20 in $5HT_3AR$ homology model [27].

Fragment affinity and selectivity cliffs

The bioactivity profiles across related and unrelated protein targets (Figure 2) allows the identification of *affinity cliffs* (two chemically similar fragments of which one is active and the other is inactive for a specific protein target) and *selectivity cliffs* (two chemically similar fragments of which one is active for a set of protein targets and the other is inactive for at least one of these targets).[53, 54] These fragment structure-activity relationships (Table 2) are illustrations of the specific interactions made at the fragment level, while they give new insights into the atomic details of (selective) protein-ligand interactions and can be used for (*in silico* guided) hit optimization. The current analysis of affinity cliffs give new insights into the atomic details of protein-ligand interactions and provide valuable information for the elucidation protein-ligand binding modes [55] for ligand optimization and design.

A couple of examples from Table 2 are highlighted to show the value of this analysis for fragment optimization strategies. Affinity cliffs involve for example changes in H-bond capacity (e.g., 1-4), basicity/acidity (e.g., 5-6) or hydrophobicity (e.g., 7-8) of functional groups. The examples in Table 2 furthermore illustrate that subtle changes in the position (9-16) or size/shape (17-20) of functional groups can influence ligand profiles. The affinity cliff resulting from the change of a cyclic amide (15) into an inverted cyclic amide (16) suggests for example a role of the amide group as an H-bond donor and/or acceptor in H_3R and H_4R. This structure-activity relationship is indeed in line with the proposed binding mode of 15 in a H_4R homology model (Figure 3d) based on the recently solved H_1R crystal structure [43] in which the amide nitrogen atom donates an H-bond to $E182^{5.46}$. This binding mode furthermore corresponds with in silico guided mutagenesis studies of H_4R, showing that the H-bond acceptor of $E182^{5.46}$ (or the glutamine mutant) is essential for binding of JNJ777120.[34, 56]

Not only *affinity* cliffs for one specific protein target can be derived from the fragment screens, but also interesting protein *selectivity* cliffs, as exemplified by the quinoxaline fragments 19 (Figure 3e) and 20 (Figure 3f). Experimentally supported docking simulations suggest that H_1R binds one of the basic diazepane nitrogen atoms of 19 via an (ionic) H-bond with its carboxylate sidechain of $D107^{3.32}$ (Figure 3e) [43], while 5HT3R binds the pyrollidine-amine of 20 and via a H-bond to the carbonyl backbone of W183, cation-π interactions with the aromatic sidechains of W183 and Y234 and a ionic interaction with E129 [46-48] (Figure 3f). Interestingly, subtle differences in the basic moiety of 19 and 20 affect binding affinity for H_1R, but not (or at least to less extend) for H_3R, H_4R, and $5HT_3R$ (Table 2).

Table 2. Examples of selectivity cliffs and switches observed in fragment library for all six targets under investigation.

Target	active	Inactive	Affinity (a)[a]/ Selectivity (s)[b] cliff
ADRB2	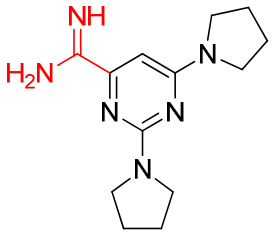	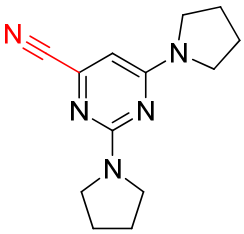	(a)
	1	2	
5-HT_3R	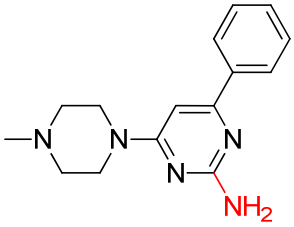	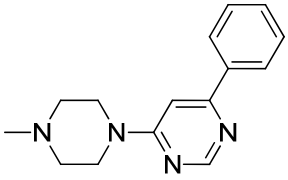	$H_1R/H_3R/H_4R$ (s)
	3	4	
H_3R/H_4R /5HT_3R	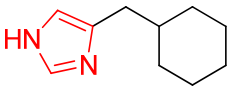	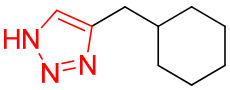	(a)
	5	6	
H_1R	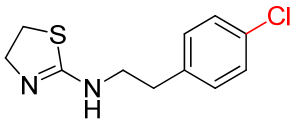	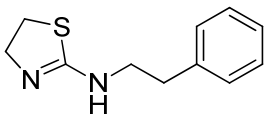	(a)
	7	8	
5-HT_3R	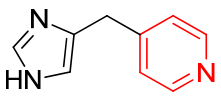	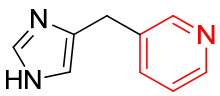	H_3R/H_4R (s)
	9	10	

5-HT$_3$R	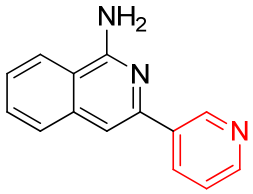	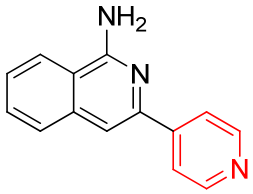	PKA-c (s)
	11	12	
PKA-c	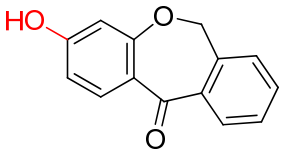	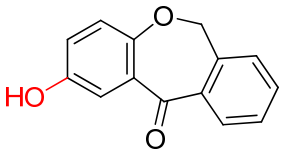	(a)
	13	14	
H$_3$R/H$_4$R	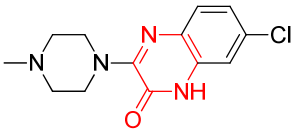	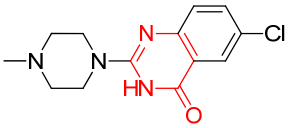	(a)
	15	16	
H$_1$R	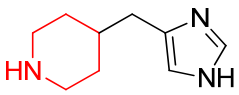	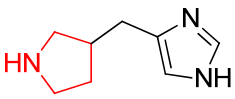	H$_3$R/H$_4$R (s)
	17	18	
H$_1$R	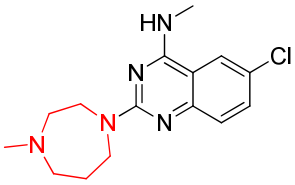	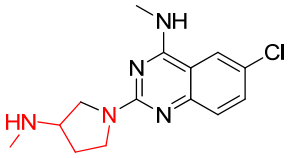	5HT$_3$R/H$_3$R/H$_4$R (s)
	19	20	

[a]*Affinity cliff: Small chemical difference in the fragment resulting in loss of binding to the target in the "Target" column [53, 54];* [b]*Selectivity cliff: Small chemical difference in the fragment resulting in loss of binding to one target (in the "Target" column), while maintaining affinity for (an)other target(s) (indicated in the "Affinity/Selectivity cliff" column) [53, 54].*

Conclusions

With fragment-based approaches on the rise, chemogenomics approaches can be fueled with data that allows a more detailed interrogation of the binding site, as illustrated in this manuscript. Accumulating studies will contribute to a better understanding of ligand-protein interaction and to the molecular features that determine ligand affinity and selectivity.

Materials and methods

Library design

Fragment structures were retrieved from the VU University's proprietary chemical database as 2D SD format and processed with the Molecular Operating Environment (MOE) software (http://www.chemcomp.com). The fragments were protonated according to the anticipated protonation states at pH=7.4; physico-chemical properties were calculated using MOE 2D descriptors. Adapted rule-of-three selection criteria were used for the filtering of fragments from our in-house compound database [16]: number of heavy atoms ≤ 22, logP < 3, number of H-bond donors ≤ 3, number of H-bond acceptors ≤ 3, number of rotatable bonds ≤ 5, number of rings ≥ 1. For the removal of compounds containing reactive functional groups, a predefined MOE descriptor was used, which is based on a published list of unwanted functionalities.[17] A scaffold diversity analysis [18] was used to evaluate the resulting first version of the fragment library.

Chemogenomics analyses

Principle components were calculated for the 28 drug-like index (DLI) descriptors.[57] The maximum of the principle components was set to three. These three components describe 51% of the DLI diversity in the library. The scaffold diversity analysis was performed in MOE, using the publicly available sca.svl script (http://svl.chemcomp.com/). Fingerprint similarity searches of two databases were performed using SciTegic's Pipeline Pilot (http://accelrys.com/products/scitegic). To define the selectivity cliffs and switches, for every strong hit (>80% displacement) the closest (with the highest fingerprint similarity score) non-active analogue was found. These hit pairs were evaluated. If these two fragments differed only one atom, and the displacement percentage differed at least 40%, the pair was defined as selectivity cliff. These cliffs were evaluated for switches with other targets.

Fragment screening assays

Screening of the fragment library on a panel of biologically relevant targets was performed with biochemical screening, using conditions comparable to HTS screening campaigns [58]. Concentrations between 200 and 10 µM were chosen. One-point affinities were determined in the different assay formats. Subsequently, hit validation experiments were conducted. Details of $5HT_{3A}R$, ADRB2, H_1R, H_3R, H_4R, and PKA-C assays been described previously.[29, 30]

References

1. de Kloe, G.E., et al., *Transforming fragments into candidates: small becomes big in medicinal chemistry.* Drug Discovery Today, 2009. **14**(13-14): p. 630-646.
2. Boyd, S.M. and G.E.d. Kloe, *Fragment library design: efficiently hunting drugs in chemical space.* Drug Discovery Today: Technologies, 2010. **7**(3): p. e173-e180.
3. Congreve, M., et al., *Recent Developments in Fragment-Based Drug Discovery.* Journal of Medicinal Chemistry, 2008. **51**(13): p. 3661-3680.
4. Erlanson, D.A., R.S. McDowell, and T. O'Brien, *Fragment-based drug discovery.* Journal of Medicinal Chemistry, 2004. **47**(14): p. 3463-3482.
5. Loving, K., I. Alberts, and W. Sherman, *Computational Approaches for Fragment-Based and De Novo Design.* Current Topics in Medicinal Chemistry, 2010. **10**(1): p. 14-32.
6. Hann, M.M., A.R. Leach, and G. Harper, *Molecular complexity and its impact on the probability of finding leads for drug discovery.* Journal of Chemical Information and Computer Sciences, 2001. **41**(3): p. 856-864.
7. Morphy, R. and Z. Rankovic, *Fragments, network biology and designing multiple ligands.* Drug Discovery Today, 2007. **12**(3-4): p. 156-160.
8. Bondensgaard, K., et al., *Recognition of privileged structures by G-protein coupled receptors.* Journal of Medicinal Chemistry, 2004. **47**(4): p. 888-899.
9. van der Horst, E., et al., *Substructure Mining of GPCR Ligands Reveals Activity-Class Specific Functional Groups in an Unbiased Manner.* Journal of Chemical Information and Modeling, 2009. **49**(2): p. 348-360.
10. Klekota, J. and F.P. Roth, *Chemical substructures that enrich for biological activity.* Bioinformatics, 2008. **24**(21): p. 2518-2525.
11. Teotico, D.G., et al., *Docking for fragment inhibitors of AmpC beta-lactamase.* Proceedings of the National Academy of Sciences of the United States of America, 2009. **106**(18): p. 7455-7460.
12. Gao, G., et al., *Identification of selective enzyme inhibitors by fragment library screening.* J Biomol Screen, 2010. **15**(9): p. 1042-50.
13. Chen, I.J. and R. Hubbard, *Lessons for fragment library design: analysis of output from multiple screening campaigns.* Journal of Computer-Aided Molecular Design, 2009.
14. Barelier, S., et al., *Ligand Specificity in Fragment-Based Drug Design.* Journal of Medicinal Chemistry, 2010. **53**(14): p. 5256-5266.
15. Leeson, P.D. and B. Springthorpe, *The influence of drug-like concepts on decision-making in medicinal chemistry.* Nature Reviews Drug Discovery, 2007. **6**(11): p. 881-890.
16. Congreve, M., et al., *A rule of three for fragment-based lead discovery?* Drug Discovery Today, 2003. **8**(19): p. 876-877.
17. Oprea, T.I., *Property distribution of drug-related chemical databases.* Journal of Computer-Aided Molecular Design, 2000. **14**(3): p. 251-264.
18. Xu, J., *A new approach to finding natural chemical structure classes.* Journal of Medicinal Chemistry, 2002. **45**(24): p. 5311-5320.
19. Siegal, G., E. Ab, and J. Schultz, *Integration of fragment screening and library design.* Drug Discovery Today, 2007. **12**(23-24): p. 1032-1039.
20. Verheij, H.J., *Leadlikeness and structural diversity of synthetic screening libraries.* Mol Divers, 2006. **10**(3): p. 377-88.
21. *Vitas-M Laboratory Ltd.* http://www.vitasmlab.com/compound-libraries/fragment-based.
22. ChEMBL, http://www.ebi.ac.uk/chembl/.
23. Wijtmans, M., et al., *Histamine H3 receptor ligands with a 3-cyclobutoxy motif: A novel and versatile constraint of the classical 3-propoxy linker.* MedChemComm, 2010. **1**(1): p. 84-86.
24. De Esch, I.J., et al., *Characterization of the binding site of the histamine H3 receptor. 1. Various approaches to the synthesis of 2-(1H-imidazol-4-yl)cyclopropylamine and histaminergic activity of (1R,2R)- and (1S,2S)-2-(1H-imidazol-4-yl)-cyclopropylamine.* J Med Chem, 1999. **42**(7): p. 1115-22.
25. Cherezov, V., et al., *High-resolution crystal structure of an engineered human beta2-adrenergic G protein-coupled receptor.* Science, 2007. **318**(5854): p. 1258-65.
26. Wawer, M. and J. Bajorath, *Similarity-potency trees: a method to search for SAR information in compound data sets and derive SAR rules.* J Chem Inf Model, 2010. **50**(8): p. 1395-409.
27. Verheij, M.H., et al., *Fragment library screening reveals remarkable similarities between the G protein-coupled receptor histamine H and the ion channel serotonin 5-HTA.* Bioorg Med Chem Lett, 2011. **21**(18): p. 5460-4.
28. Thompson, A.J., et al., *An efficient and information-rich biochemical method design for fragment library screening on ion channels.* Biotechniques, 2010. **49**(5): p. 822-829.
29. Sanders, M.P.A., et al., *A Prospective Cross-Screening Study on G Protein-Coupled Receptors: Lessons Learned in Virtual Compound Library Design.* Under revision, 2012.
30. de Graaf, C., et al., *Crystal structure-based virtual screening for fragment-like ligands of the human histamine H(1) receptor.* J Med Chem, 2011. **54**(23): p. 8195-206.

31. Istyastono, E.P., et al., *Molecular determinants of selective agonist and antagonist binding to the histamine H4 receptor.* Current Topics in Medicinal Chemistry, 2010. **In press.**
32. Celanire, S., et al., *Keynote review: histamine H3 receptor antagonists reach out for the clinic.* Drug Discov Today, 2005. **10**(23-24): p. 1613-27.
33. Smits, R.A., R. Leurs, and I.J. de Esch, *Major advances in the development of histamine H4 receptor ligands.* Drug Discov Today, 2009. **14**(15-16): p. 745-53.
34. Jongejan, A., et al., *Delineation of agonist binding to the human histamine H4 receptor using mutational analysis, homology modeling, and ab initio calculations.* J Chem Inf Model, 2008. **48**(7): p. 1455-63.
35. Shin, N., et al., *Molecular modeling and site-specific mutagenesis of the histamine-binding site of the histamine H4 receptor.* Mol Pharmacol, 2002. **62**(1): p. 38-47.
36. Istyastono, E.P., et al., *Molecular determinants of ligand binding modes in the histamine H(4) receptor: linking ligand-based three-dimensional quantitative structure-activity relationship (3D-QSAR) models to in silico guided receptor mutagenesis studies.* J Med Chem, 2011. **54**(23): p. 8136-47.
37. Shamovsky, I., et al., *Increasing selectivity of CC chemokine receptor 8 antagonists by engineering nondesolvation related interactions with the intended and off-target binding sites.* J Med Chem, 2009. **52**(23): p. 7706-23.
38. Leeson, P.D. and B. Springthorpe, *The influence of drug-like concepts on decision-making in medicinal chemistry.* Nat Rev Drug Discov, 2007. **6**(11): p. 881-90.
39. Ohta, K., et al., *Site-directed mutagenesis of the histamine H1 receptor: roles of aspartic acid107, asparagine198 and threonine194.* Biochem Biophys Res Commun, 1994. **203**(2): p. 1096-101.
40. Bruysters, M., et al., *Mutational analysis of the histamine H1-receptor binding pocket of histaprodifens.* Eur J Pharmacol, 2004. **487**(1-3): p. 55-63.
41. Leurs, R., et al., *Site-directed mutagenesis of the histamine H1-receptor reveals a selective interaction of asparagine207 with subclasses of H1-receptor agonists.* Biochem Biophys Res Commun, 1994. **201**(1): p. 295-301.
42. Wieland, K., et al., *Mutational analysis of the antagonist-binding site of the histamine H(1) receptor.* J Biol Chem, 1999. **274**(42): p. 29994-30000.
43. Shimamura, T., et al., *Structure of the human histamine H1 receptor complex with doxepin.* Nature, 2011. **475**(7354): p. 65-70.
44. Surgand, J.S., et al., *A chemogenomic analysis of the transmembrane binding cavity of human G-protein-coupled receptors.* Proteins-Structure Function and Bioinformatics, 2006. **62**(2): p. 509-538.
45. Katritch, V., V. Cherezov, and R.C. Stevens, *Diversity and modularity of G protein-coupled receptor structures.* Trends Pharmacol Sci, 2012. **33**(1): p. 17-27.
46. Price, K.L., et al., *A Hydrogen Bond in Loop A Is Critical for the Binding and Function of the 5-HT3 Receptor.* Biochemistry, 2008.
47. Price, K.L. and S.C. Lummis, *The role of tyrosine residues in the extracellular domain of the 5-hydroxytryptamine3 receptor.* J Biol Chem, 2004. **279**(22): p. 23294-301.
48. Beene, D.L., et al., *Cation-pi interactions in ligand recognition by serotonergic (5-HT3A) and nicotinic acetylcholine receptors: the anomalous binding properties of nicotine.* Biochemistry, 2002. **41**(32): p. 10262-9.
49. Ghose, A.K., et al., *Knowledge based prediction of ligand binding modes and rational inhibitor design for kinase drug discovery.* J Med Chem, 2008. **51**(17): p. 5149-71.
50. Yang, Y., et al., *Investigation of the Relationship between Topology and Selectivity for Druglike Molecules.* J Med Chem, 2010. **53**(21): p. 7709-14.
51. Hopkins, A.L., J.S. Mason, and J.P. Overington, *Can we rationally design promiscuous drugs?* Current Opinion in Structural Biology, 2006. **16**(1): p. 127-136.
52. Shi, L. and J.A. Javitch, *The binding site of aminergic G protein-coupled receptors: the transmembrane segments and second extracellular loop.* Annu Rev Pharmacol Toxicol, 2002. **42**: p. 437-67.
53. Stumpfe, D. and J. Bajorath, *Exploring activity cliffs in medicinal chemistry.* J Med Chem, 2012. **55**(7): p. 2932-42.
54. Bajorath, J., *Modeling of activity landscapes for drug discovery.* Expert Opin Drug Discov, 2012. **7**(6): p. 463-73.
55. de Graaf, C. and D. Rognan, *Customizing G Protein-coupled receptor models for structure-based virtual screening.* Curr Pharm Des, 2009. **15**(35): p. 4026-48.
56. Lim, H.D., et al., *Molecular determinants of ligand binding to H4R species variants.* Mol Pharmacol, 2010. **77**(5): p. 734-43.
57. Tang, K., et al., *Discrimination of approved drugs from experimental drugs by learning methods.* BMC Bioinformatics, 2011. **12**: p. 157-163.
58. Pereira, D.A. and J.A. Williams, *Origin and evolution of high throughput screening.* British Journal of Pharmacology, 2007. **152**(1): p. 53-61.